Clinical Infectious Diseases

MAJOR ARTICLE

The Diagnostic Accuracy of Chest Radiographic Features for Pediatric Intrathoracic Tuberculosis

Megan Palmer,[1] Kenneth S. Gunasekera,[2] Marieke M. van der Zalm,[1] Julie Morrison,[3] H. Simon Schaaf,[1,3] Pierre Goussard,[3] Anneke C. Hesseling,[1] Elisabetta Walters,[1,4,a] and James A. Seddon[1,5,a]

[1]Desmond Tutu TB Centre, Department of Pediatrics and Child Health, Faculty of Medicine and Health Sciences, Stellenbosch University, Cape Town, South Africa; [2]Department of Epidemiology of Microbial Diseases, Yale School of Public Health, New Haven, Connecticut, USA; [3]Department of Pediatrics and Child Health, Faculty of Medicine and Health Sciences, Stellenbosch University, Cape Town, South Africa; [4]Great North Children's Hospital, Newcastle upon Tyne Hospitals Trust, Newcastle, United Kingdom; and [5]Department of Infectious Diseases, Imperial College London, London, United Kingdom

Introduction. The chest radiograph (CR) remains a key tool in the diagnosis of pediatric tuberculosis (TB). In children with presumptive intrathoracic TB, we aimed to identify CR features that had high specificity for, and were strongly associated with, bacteriologically confirmed TB.

Methods. We analyzed CR data from children with presumptive intrathoracic TB prospectively enrolled in a cohort study in a high-TB burden setting and who were classified using standard clinical case definitions as "confirmed," "unconfirmed," or "unlikely" TB. We report the CR features and inter-reader agreement between expert readers who interpreted the CRs. We calculated the sensitivity and specificity of the CR features with at least moderate inter-reader agreement and analyzed the relationship between these CR features and the classification of TB in a multivariable regression model.

Results. Of features with at least moderate inter-reader agreement, enlargement of perihilar and/or paratracheal lymph nodes, bronchial deviation/compression, cavities, expansile pneumonia, and pleural effusion had a specificity of > 90% for confirmed TB, compared with unlikely TB. Enlargement of perihilar (adjusted odds ratio [aOR]: 6.6; 95% confidence interval [CI], 3.80–11.72) and/or paratracheal lymph nodes (aOR: 5.14; 95% CI, 2.25–12.58), bronchial deviation/compression (aOR: 6.22; 95% CI, 2.70–15.69), pleural effusion (aOR: 2.27; 95% CI, 1.04–4.78), and cavities (aOR: 7.45; 95% CI, 3.38–17.45) were associated with confirmed TB in the multivariate regression model, whereas alveolar opacification (aOR: 1.16; 95% CI, .76–1.77) and expansile pneumonia (aOR: 4.16; 95% CI, .93–22.34) were not.

Conclusions. In children investigated for intrathoracic TB enlargement of perihilar or paratracheal lymph nodes, bronchial compression/deviation, pleural effusion, or cavities on CR strongly support the diagnosis.

Keywords. pediatric; children; tuberculosis; chest x-ray; radiograph.

Of the 1.5 million tuberculosis (TB) deaths in 2020, 16% were children < 15 years [1]. This is a disproportionate burden given that pediatric TB comprises 11% of all TB and that TB outcomes for children who receive treatment are good [2–7]. This mortality can be largely attributed to poor access to TB diagnosis and treatment—only an estimated 41% of children with TB access treatment and modelling studies show that 95% of children who die from TB are undiagnosed at the time of death [1, 8]. Improving diagnostic strategies for pediatric TB is a priority.

In the absence of a globally accessible, adequately accurate diagnostic test for TB in children, which is typically paucibacillary, the diagnosis remains largely clinical and based on symptoms and history. More than 75% of pediatric TB is intrathoracic and the chest radiograph (CR) is central to diagnostic decision-making [9–11]. CRs are widely available, even in resource-limited settings, and pose minimal radiation risk. In the context of diagnostic algorithms, CRs are usually placed after the assessment of symptoms, signs, and TB exposure history. Gunasekera and colleagues recently demonstrated that including CR interpretation, in addition to clinical information, in diagnostic algorithms for children evaluated for intrathoracic TB increased the proportion of TB cases identified [12]. Although the "classical" CR features of intrathoracic TB are widely accepted (enlargement of mediastinal lymph nodes, large airway compression, cavitary disease, miliary infiltrates, Ghon complex/focus, pleural effusion, consolidation/collapse), using these individual CR features to inform the overall assessment of radiological diagnostic certainty ("suggestive of" or "consistent with" TB) is not standardized and is based largely on expert opinion rather than on empirical data [13–15]. CR interpretation in children is complicated by the broad radiological disease spectrum and substantial variation in radiological patterns by age, human

Received 22 October 2021; editorial decision 3 January 2022; published online 7 January 2022.
[a]E. W. and J. A. S. are joint senior authors.
Correspondence: M. Palmer, Desmond Tutu TB Centre, Department of Pediatrics and Child Health, Faculty of Medicine and Health Sciences, Stellenbosch University, Francie Van Zyl Drive, Parow, Cape Town 7505, South Africa (meganpalmer@sun.ac.za).

Clinical Infectious Diseases® 2022;75(6):1014–21

https://doi.org/10.1093/cid/ciac011

immunodeficiency virus (HIV) status, and presence of other comorbidities, such as viral/bacterial lower respiratory tract coinfection [10, 16–20].

CRs classified broadly as "suggestive" or "not suggestive of" intrathoracic TB have suboptimal sensitivity and specificity [21, 22]. The few studies that report the diagnostic performance of individual CR features for pediatric TB suggest that individual features or combinations thereof may be more informative. Berteloot and colleagues identified key CR features (a Ghon focus, miliary infiltrates, enlargement of paratracheal lymph nodes, cavities, nodular opacities, large airway compression, and pleural effusion) with > 90% specificity for confirmed intrathoracic TB in children living with HIV, and Richter-Joubert and colleagues demonstrated that large airway compression on CR was strongly associated with confirmed TB in young children [23, 24].

Including the presence of individual CR features that have quantifiable diagnostic performance, rather than a single binary variable of overall radiological certainty in diagnostic algorithms, may improve their utility. We describe individual CR features from a well-characterized cohort of young children presenting to care and systematically investigated for intrathoracic TB. After excluding CR features with poor concordance between readers, we calculated the sensitivity and specificity of individual CR features for confirmed TB and then analyzed these features in a multivariable regression model.

METHODS

Study Setting

This study was conducted at a district level and a tertiary referral hospital in Cape Town, South Africa. The burden of TB in this area is high; estimated incidence of 730 per 100 000 [25].

Design and Study Population

Data were collected as part of a prospective diagnostic study in children investigated for intrathoracic TB [26]. Children were eligible for inclusion if they were < 13 years of age and had presented with presumptive intrathoracic TB to a hospital between April 2012 and March 2017. Presumptive TB was defined as either having well-defined symptoms of TB, or presenting with acute symptoms (< 2 weeks) and other additional risk factors for TB disease. Well-defined symptoms were ≥ 1 of: (1) cough ≥ 2 weeks; (2) unexplained fever ≥ 1 week; or (3) documented poor growth or weight loss over the preceding 3 months. Additional risk factors were: (1) contact with an adult TB source case; (2) a positive tuberculin skin test (TST, 2 tuberculin units PPD RT-23, Statens Serum Institute, Copenhagen): > 10 mm in HIV-negative and > 5 mm in HIV-positive children; or (3) a CR considered by routine attending clinicians as suggestive of TB.

All children had the following investigations at study entry (baseline): CR (anteroposterior [AP] or posteroanterior [PA] and lateral views), TST, and collection of 2–4 respiratory specimens tested using fluorescent auramine smear microscopy, Xpert MTB/RIF (Xpert, Cepheid, Sunnyvale, CA) and liquid Mycobacterial Growth Indicator Tube (Becton Dickinson, Sparks, MD, USA) culture (Supplementary Table 1).

The decision to start TB treatment was made by routine attending clinicians. All children were followed regularly to 6 months to assess their clinical and radiological response to treatment and to review mycobacterial culture and other results. Participants were retrospectively classified by the research team, using standard clinical case definitions for intrathoracic TB, as "confirmed TB," "unconfirmed TB," or "unlikely TB" (not TB) [11]. Baseline CRs from children were included in this analysis if an AP/PA film classified as being of acceptable quality by 2 readers was available for review and if clinical information from the participant was sufficiently complete for clinical classification.

The study was approved by the Stellenbosch University Health Research Ethics Committee (N11/09/282), local hospitals, and the provincial Department of Health.

Methods of CR Reading and Radiological Classification

CRs were digital and were captured on a Philips iSite Picture Archiving and Communications System. CRs were independently read by at least 2 experienced pediatricians (2 pediatric pulmonologists and 1 pediatric TB specialist) using a standard CR reading form. Readers were blinded to clinical details, laboratory results, and to the other readers' CR reading. For this analysis, the first 2 individual CR reads were included so that each CR from each child generated 2 CR reads and the number of CR reads was double the number of child cases.

Each CR was systematically classified by each CR reader (Supplementary Figure 1) as being of "acceptable" or "unacceptable" quality. If acceptable quality, then as being "normal" or "abnormal." If any of the following individual CR features were present the CR was classified as "abnormal": alveolar consolidation, bronchopneumonia, interstitial infiltrates, collapse, miliary infiltrates, Ghon focus, cavities, perihilar infiltrates, enlarged perihilar (including subcarinal) or paratracheal lymph nodes, bronchial and/or tracheal compression/deviation, and pleural effusion. The option of "uncertain" was available for the presence of enlarged perihilar and paratracheal lymph nodes only. CR data are presented per CR read and not per participant.

Statistical Analysis

Analyses were carried out using R version 4.0.5 (The R Foundation for Statistical Computing). Clinical and demographic features are presented by diagnostic category. Perihilar or paratracheal lymph nodes classified as "uncertain" were excluded from analysis. Results are stratified by age < 2 years, 2 to < 5 years and ≥ 5 years.

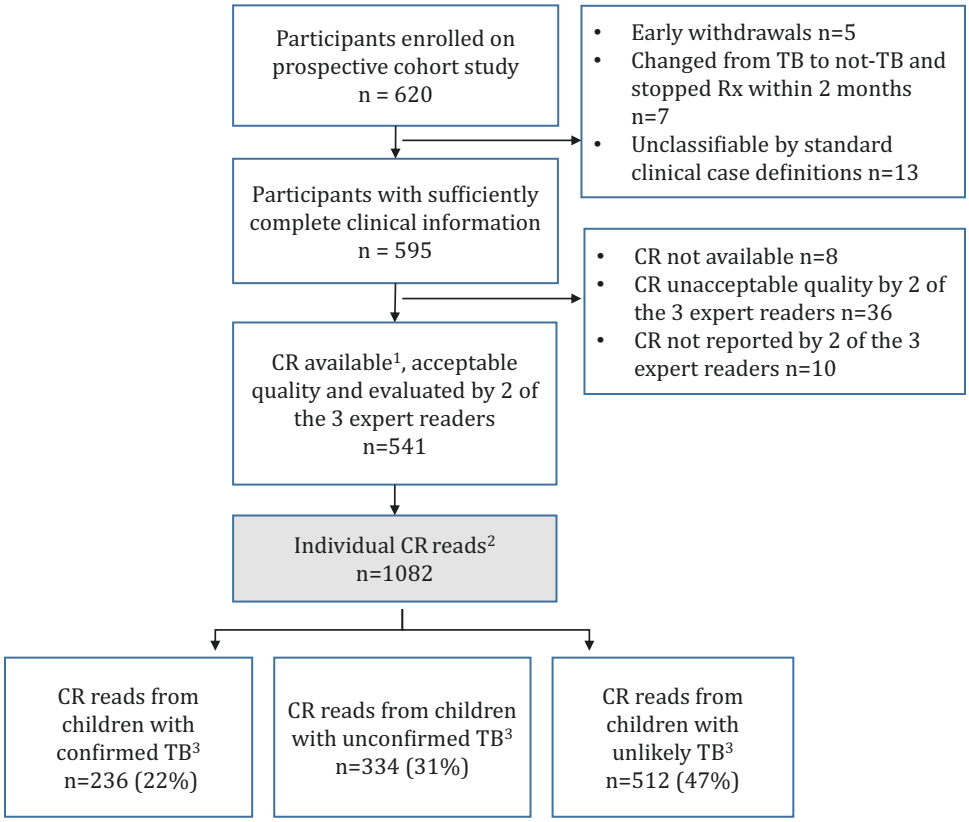

Figure 1. Overview of child participants and chest radiographs included in this analysis.
CR, chest radiograph; Rx, treatment; TB, tuberculosis.
[1]CR read based on assessment of anteroposterior or posteroanterior film with/without lateral film.
[2]Each child had 1 CR and each CR generated 2 individual CR reads, so that the number of CR reads was double the number of CRs and double the number of child cases.
[3]Confirmed, unconfirmed, and unlikely intrathoracic TB as per standard clinical case definitions (Graham et al. [11]).

Inter-reader agreement was calculated using Cohen kappa coefficient (k) using the *kappa2.table* function in the package *irrCAC* [27], presented with 95% confidence intervals (CIs), classified as follows: ≤0 no agreement, 0.01–0.2 slight, 0.21–0.4 fair, 0.41–0.6 moderate, 0.61–0.8 substantial, and 0.81–1.00 almost perfect agreement. UpSet plots were used to present combinations of CR features using the *upset* function in the package *UpSetR* [28].

We propose that only CR features readers can identify with confidence will be clinically useful and therefore excluded CR features with less than moderate agreement between 2 (of 3) reader pairs from the estimates of sensitivity and specificity and the regression model. Both the sensitivity and specificity estimates and the regression model were restricted to children with confirmed and unlikely TB.

RESULTS

Study Population

In total, 620 children were enrolled into the diagnostic study; CRs from 541 children were included in this analysis. Each child had 1 baseline CR (AP/PA ± lateral CR) taken, which generated 2 individual CR reads; 1082 CR reads were analyzed (Figure 1).

The median age was 16.9 (interquartile range 9.8–33.5) months; 485 (90%) children were ≤ 5 years. Sixty-eight (13%) children were living with HIV and 285 (53%) were retrospectively determined to have intrathoracic TB using standard clinical case definitions (41% microbiologically confirmed and 59% unconfirmed, Table 1).

Frequency of CR Features and Inter-Reader Agreement

Overall, the most common CR features among the 236 CR reads from children with confirmed intrathoracic TB were alveolar opacification (118/236; 50%), enlarged perihilar lymph nodes (100/236; 42%), bronchial deviation/compression (69/236; 29%), and enlarged paratracheal lymph nodes (54/236; 23%). Among the 512 CR reads from children with unlikely intrathoracic TB, 139 (27%) had normal CRs. The most common CR abnormalities in this group were alveolar opacification (181/512; 35%) and perihilar infiltrates (132/512; 26%; Table 2). Supplementary Table 2 show the frequency of radiological features by clinical case definitions and age.

Table 1. Baseline Demographics and Clinical Characteristics of Children by Clinical Case Definitions for Intrathoracic Tuberculosis

	Overall, n or median (% or IQR)	Confirmed TB, n or median (% or IQR)	Unconfirmed TB, n or median (% or IQR)	Unlikely TB, n or median (% or IQR)
Number	541	118	167	256
Age (mo) overall	16.9 (9.8–33.5)	22.2 (9.9–52.1)	17.2 (10.7–29.4)	15.3 (9.3–28.6)
<2 y	343 (63)	61 (52)	110 (66)	172 (67)
2–5 y	142 (26)	33 (28)	43 (26)	66 (26)
>5 y	56 (10)	24 (20)	14 (8)	18 (7)
Female	256 (47)	67 (57)	72 (43)	117 (46)
HIV exposed	89 (16)	20 (17)	29 (17)	40 (16)
HIV positive	68 (13)	17 (14)	30 (18)	21 (8)
WAZ	−1.68 (−2.73 to −0.73)	−1.86 (−2.91 to −0.91)	−1.73 (−3.07 to −0.62)	−1.52 (−2.61 to −0.74)
HAZ (n = 526)	−1.77 (−2.92 to −0.63)	−1.86 (−2.97 to −0.63)	−1.62 (−3.09 to −0.62)	−1.72 (−2.8 to −0.64)
Documented TB exposure	202 (37)	56 (47)	89 (53)	57 (22)
TST positive	115/403[a] (29)	58/83[a] (70)	43/129[a] (33)	14/191[a] (7)

Abbreviations: HAZ, height-for-age z-score; IQR, interquartile range; WAZ, weight-for-age z-score; TB, tuberculosis; TST, tuberculin skin test; HIV, human immunodeficiency virus

[a]TST could not be administered to all children because of a national tuberculin stock-out; denominator represents total number of children who had a TST placed within each subgrouping.

CRs from children with confirmed TB had more abnormal features and more combinations of abnormal CR features (34 different combinations compared with 16 and 13 combinations from children with unconfirmed and unlikely TB, respectively). Although alveolar consolidation was the most frequently reported CR feature across all clinical case categories, this was more frequently the only abnormality on CR in children with unlikely TB (116/150; 77%) compared with confirmed TB (26/100; 26%) (Figure 2).

Each CR was interpreted by 2 of 3 expert readers and there was moderate to substantial inter-reader agreement (kappa > 0.4) between all 3 combinations of 2-reader pairs for the presence of alveolar consolidation, pleural effusion, expansile pneumonia, and enlarged perihilar lymph nodes, and between 2 of the 3 reader combination pairs for cavities, enlarged paratracheal lymph nodes, and bronchial compression/deviation (Table 3). Inter-reader agreement was poorest for bronchopneumonia and interstitial infiltrates, with highest kappa of 0.27 (-0.07 to 0.61) and 0.29 (0.11–0.46), respectively. Inter-reader agreement stratified by age is shown in Supplementary Table 3.

Diagnostic Performance of Individual CR Features

For CR features with at least moderate inter-reader agreement and when comparing confirmed TB with unlikely TB, enlarged

Table 2. Frequency of Chest Radiograph Features by Standard Clinical Case Definitions in Children Investigated for Intrathoracic Tuberculosis

	Overall, n (%)	Confirmed TB, n (%)	Unconfirmed TB, n (%)	Unlikely TB, n (%)	*P* value[b]
Number of CR reads[a]	1082	236	334	512	
Any abnormality	884 (82)	225 (95)	286 (86)	373 (73)	<.05
Alveolar opacification	422 (39)	118 (50)	123 (37)	181 (35)	<.05
Bronchopneumonia	144 (13)	35 (15)	51 (15)	58 (11)	.19
Collapse	79 (7)	15 (6)	21 (6)	43 (8)	.38
Perihilar infiltrates	254 (23)	40 (17)	82 (25)	132 (26)	<.05
Interstitial infiltrates	96 (9)	8 (3)	42 (13)	46 (9)	<.05
Enlarged perihilar lymph nodes[c]	186 (17)	100 (42)	61 (18)	25 (5)	<.05
Enlarged paratracheal lymph nodes[c]	91 (8)	54 (23)	27 (8)	10 (2)	<.05
Tracheal deviation/compression	27 (2)	22 (9)	3 (<1)	2 (<1)	<.05
Bronchial deviation/compression	100 (9)	69 (29)	22 (7)	9 (2)	<.05
Miliary infiltrates	23 (2)	15 (6)	7 (2)	1 (<1)	<.05
Ghon focus	18 (2)	9 (4)	6 (2)	3 (<1)	<.05
Cavities	61 (6)	32 (14)	17 (5)	12 (2)	<.05
Expansile pneumonia	16 (1)	12 (5)	1 (<1)	3 (<1)	<.05
Pleural effusion	57 (5)	21 (9)	14 (4)	22 (4)	<.05

Abbreviations: CR, chest radiograph; TB, tuberculosis.

[a]Each CR generated 2 single independent CR reads (each read was based on assessment of anteroposterior or posteroanterior film with/without lateral film).

[b]*P* values calculated using Fisher exact test to compare the groups confirmed and unlikely TB.

[c]Perihilar or paratracheal lymph nodes classified as "uncertain" were excluded.

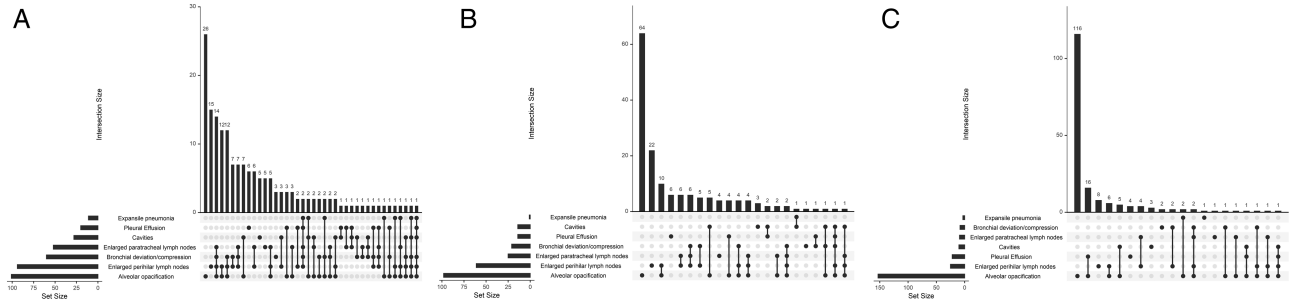

Figure 2. UpSet diagrams illustrating the reported number of isolated chest radiograph features and most frequent combinations of chest radiograph features by clinical TB case definitions for intrathoracic TB.[a]

(A) Confirmed Intrathoracic TB, (B) Unconfirmed Intrathoracic TB, (C) Unlikely Intrathoracic TB.

The horizontal bar charts on the bottom show the number of CRs where the select CR feature was present, whereas the vertical bar charts illustrate how often the CR feature was seen as the only isolated abnormality on the film (illustrated as single dot) and in combination with other abnormal CR features (illustrated as multiple connected dots). For CR reads where perihilar or paratracheal lymph nodes were classified as "uncertain," the entire CR read was excluded from this representation.

Abbreviations: CR, chest radiograph; TB, tuberculosis.

[a]Graham et al. [11].

perihilar and paratracheal lymph nodes, bronchial deviation/compression, cavities, expansile pneumonia, and pleural effusion had high specificity (90%) but poor sensitivity (<50%) for confirmed TB across all age groups. "Any abnormality" (CR classified as "abnormal" by the reader) on CR was the only feature with sensitivity > 90% (Table 4).

Multivariable Model

In multivariable regression, including only features with at least moderate inter-reader agreement, enlarged perihilar lymph nodes (adjusted odds ratio [aOR]: 6.62; 95% CI, 3.80–11.72), enlarged paratracheal lymph nodes (aOR: 5.14; 95% CI, 2.25–12.58), bronchial compression/deviation (aOR: 6.22; 95% CI, 2.70–15.69), pleural effusion (aOR: 2.27; 95% CI, 1.04–4.78), and cavities (aOR: 7.45; 95% CI, 3.38–17.45) were associated with confirmed TB ; expansile pneumonia (aOR: 4.16; 95% CI, .93–22.34) and alveolar opacification (aOR: 1.16; 95% CI, .76–1.77) were not (Table 5).

DISCUSSION

When CRs are read in a way that results in a binary radiological classification ("suggestive of TB" vs "not suggestive of TB"), sensitivity and specificity is suboptimal [21, 22]. However, we found that there are individual CR features with good inter-reader agreement that have high specificity for, and are

Table 3. Inter-Reader Agreement Between Expert Readers for the Presence of Individual Chest Radiograph Features in Children Investigated for Intrathoracic TB

	All		
	Reader 1 and 2 k, (95% CI)	Reader 1 and 3, k (95% CI)	Reader 2 and 3, k (95% CI)
Number of CR reads[a]	259	162	120
Any abnormality	0.55 (.41–.68)	0.55 (.40–.71)	0.46 (.25–.67)
Alveolar opacification	0.47 (.37–.56)	0.52 (.39–.66)	0.47 (.31–.63)
Bronchopneumonia	0.10 (-.01–.21)	0.15 (.01–.29)	0.27 (-.07–.61)
Collapse	0.52 (.34–.71)	-0.01 (-.03– .01)	0.26 (-.05– .56)
Perihilar infiltrates	0.20 (.10–.30)	0.26 (.07–.44)	0.37 (.19–.55)
Interstitial infiltrates	0.29 (.11–.46)	-0.01 (-.16–.15)	0.08 (-.13–.31)
Enlarged perihilar lymph nodes	0.52 (.39–.65)	0.62 (.47–.78)	0.64 (.39–.89)
Enlarged paratracheal lymph nodes	0.41 (.24–58)	0.35 (.10–.61)	0.79 (.51–1.0)
Tracheal deviation/compression	0.33 (.03–.63)	0.27 (-.17–.72)	0.01 (-.03–.01)
Bronchial deviation/compression	0.54 (.38–.70)	0.37 (.13–.60)	0.79 (.51–1.0)
Miliary infiltrates	0.38 (.06–.70)	0.56 (.11–1.0)	0.00 (.0–.0)
Ghon focus	0.32 (-.03–.67)	0.66 (.04–1.0)	0.01 (-.03–.01)
Cavities	0.42 (.21–.62)	0.34 (-.02– .71)	0.91 (.72–1.0)
Expansile pneumonia	0.49 (.06–.92)	1.0 (1.0–1.0)	0.49 (-.12– 1.0)
Pleural effusion	0.43 (.19–.68)	0.75 (.53–.96)	0.79 (.51–1.0)

Interpretation of Cohen kappa coefficient: ≤0 no agreement, 0.01–0.2 slight agreement, 0.21–0.4 fair agreement, 0.41–0.6 moderate agreement, 0.61–0.8 substantial agreement, 0.81–1.00 almost perfect agreement.

Abbreviations: CI, confidence interval; CR, chest radiograph; k, Cohen kappa coefficient.

[a]Each CR generated 2 single independent CR reads.

Table 4. Diagnostic Accuracy of Chest Radiograph Features for Confirmed Intrathoracic Tuberculosis in Children by Age

	All				<2 y				2 to < 5 y				≥5 y			
	N = 748				N = 466				N = 198				N = 84			
		Sensitivity		Specificity		Sensitivity		Specificity		Sensitivity		Specificity		Sensitivity		Specificity
	n (%)	% 95% CI		% 95% CI	n (%)	% 95% CI		% 95% CI	n (%)	% 95% CI		% 95% CI	n (%)	% 95% CI		% 95% CI
Any abnormality	598 (80)	95 (93–98)		27 (21–33)	379 (81)	96 (92–99)		24 (16–31)	158 (80)	95 (90–100)		28 (17–39)	61 (73)	94 (87–100)		56 (41–70)
Alveolar opacification	299 (40)	55 (44–56)		65 (59–71)	187 (40)	49 (40–58)		63 (55–72)	76 (38)	50 (38–62)		67 (56–79)	36 (43)	52 (38–66)		69 (56–82)
Enlarged perihilar lymph nodes	64 (9)	28 (39–52)		95 (92–98)	79 (17)	53 (44–62)		94 (90–99)	36 (19)	48 (36–61)		94 (89–100)	10 (12)	21 (10–33)		100
Enlarged paratracheal lymph nodes	125 (17)	24 (19–30)		98 (96–100)	40 (9)	27 (19–35)		97 (94–100)	14 (7)	21 (11–31)		99 (97–100)	10 (12)	21 (10–33)		100
Bronchial deviation/ compression	78 (10)	29 (23–35)		98 (97–100)	61 (13)	43 (35–52)		98 (95–100)	14 (7)	20 (10–29)		99 (97–100)	3 (4)	6 (0–13)		94 (99–100)
Cavities	44 (6)	8 (9–18)		98 (96–100)	22 (5)	11 (6–17)		98 (95–100)	6 (3)	6 (0–12)		98 (96–100)	16 (19)	29 (16–42)		100
Expansile pneumonia	15 (2)	5 (2–8)		99 (98–100)	10 (2)	7 (3–12)		100	5 (3)	5 (0–10)		98 (96–100)	0	0		100
Pleural effusion	43 (6)	9 (5–13)		96 (94–98)	21 (5)	4 (1–8)		95 (92–99)	16 (8)	15 (7–24)		95 (99–100)	6 (7)	13 (3–22)		100

This analysis was restricted to CR reads from children with confirmed and unlikely intrathoracic TB; confirmed TB was used as the diagnostic reference standard.

Abbreviations: CI, confidence interval; CR, chest radiograph; TB, tuberculosis.

strongly associated with, confirmed intrathoracic TB. When investigating a child with presumptive intrathoracic TB in a high-TB burden setting, enlargement of mediastinal lymph nodes, bronchial compression, pleural effusion, and cavities on CR strongly support the diagnosis. Alveolar consolidation, frequently reported in children with intrathoracic TB, is usually seen in combination with other CR features and, as an isolated feature, does not distinguish children with confirmed TB from children with unlikely TB.

The pattern of CR abnormalities seen in children with unconfirmed TB differs from those with confirmed TB, with lower frequency of features with high specificity for TB (Table 2). We propose that children with unconfirmed TB in this study may have presented earlier (with lower bacterial burden as evidenced by absence of microbiological confirmation) and less advanced radiological disease. Enlarged mediastinal lymph nodes, bronchial compression, and expansile pneumonia are more sensitive features for intrathoracic TB in the youngest age group compared with the oldest, with the converse being true of pleural effusion and cavitary disease (Table 4). This may be a reflection of the variation in prevalence of these CR features by age. Interpretation of results stratified by age should be made with caution, however, as CR numbers in each subgroup are small.

The inter-reader agreement for CR features presented in this study is better than in other studies. Kappas for inter-reader agreement on the presence of enlarged mediastinal lymph nodes and large airway compression (reported in previous studies as < 0.4 and < 0.3, respectively) were > 0.4 and 0.37–0.79 for all reader pairs in our study [23, 29]. The CR readers in previous comparative studies were similarly qualified to our readers. Concordance may have been higher in our study because the readers had worked in the same department for several years. We did not identify consistent differences in concordance between reader pairs (ie, 1 reader pair consistently agreeing more than another); this may reflect a combination of technical limitations of the CR as well as the subjectivity of the observer. This variability in interpretation remains a limitation of CR. Because CR quality may vary by age and poor CR quality complicates interpretation, we analyzed inter-reader agreement for CR features from children stratified by age group. We did not see consistently poorer concordance between CR reads from younger children compared with older children. For pleural effusion, however, where the overall concordance was lower than expected, concordance was best in children ≥ 5 years of age (Supplementary Table 3). This may be explained by the fact that pleural effusions in older children were more commonly an isolated CR feature (9/15, 60%) compared with those in younger children (3/42, 7%), where effusions were commonly associated with other CR abnormalities, which may complicate interpretation.

In the absence of a sensitive and accurate diagnostic test, there is no perfect reference standard in pediatric TB. The following options are available: (1) an imaging reference standard such as

Table 5. Multivariate Analysis Using Logistical Regression to Identify Which Chest Radiograph Features Are Associated With Having Confirmed Intrathoracic Tuberculosis

	Unadjusted OR	95% CI	Adjusted OR	95% CI
Enlarged perihilar lymph nodes	15.85	9.31–24.49	6.62	3.80–11.72
Enlarged paratracheal lymph nodes	15.76	8.19–33.48	5.14	2.25–12.58
Bronchial compression/ deviation	23.09	11.88–50.56	6.22	2.70–15.69
Alveolar opacification	1.83	1.34–2.50	1.16	0.76–1.77
Cavity	6.54	3.39–13.44	7.45	3.38–17.45
Pleural effusion	2.28	1.17–4.05	2.27	1.04–4.78
Expansile pneumonia	9.09	2.85–40.18	4.16	0.93–22.34

This analysis was restricted to CR reads from children with confirmed and unlikely TB.

Abbreviations: CI, confidence interval; CR, chest radiograph; OR, odds ratio; TB, tuberculosis.

chest computed tomography (CT); (2) a microbiological reference standard (culture and/or Xpert MTB/RIF-confirmed TB); or (3) a clinical reference standard. Chest CT was not included in the study from which these data were collected. We considered microbiologically confirmed TB as the most robust (and widely accepted) reference standard and this was used in the estimates of sensitivity and specificity and the multivariable regression model. The clinical reference standards of confirmed, unconfirmed, and unlikely intrathoracic TB [11] were established specifically for pediatric TB diagnostic studies and are widely accepted in the literature. However, we elected not to use the clinical reference standard of unconfirmed TB (alone or in combination with confirmed TB) in this study because a "CR consistent with TB" is a key criterion for this case definition and we believed that comparing CR features against this reference was methodologically flawed. We acknowledge that there may be similar limitations to using unlikely TB as the "control" reference standard. However, having a well-classified group of children who presented with similar symptomatology as children ultimately classified as having TB, who were not treated for TB and remained well during follow-up, was appropriate despite these limitations.

Few published studies report on the performance of individual CR features for the diagnosis of pediatric intrathoracic TB. The CR features reported here with > 90% specificity for confirmed TB performed similarly in an analysis by Berteloot and colleagues, except for perihilar lymph nodes, which had considerably higher specificity in our analysis [22]. The children in the Berteloot cohort all had HIV and were older (median age 7.25 years) and CR features were established after a consensus read with poorer inter-reader agreement; these factors limit comparison. The aOR of 6.22 (2.70–15.69) for bronchial compression in our study was similar to the aOR of 6.02 (3.45–10.51) for any large airway compression reported from a South African hospital-based cohort similar to ours [24].

This study is strengthened by the fact that the CRs were taken from a well-characterized large cohort of children with high culture confirmation rates and long-term clinical follow-up, and well-characterized controls without TB, allowing for robust case classification. This large CR dataset had high-quality digital images, lateral films in > 90%, and CR findings were systematically recorded in a blinded manner by experienced readers using standard forms.

Our study has limitations. The cohort was young and hospital-based and their CRs may not be representative of all children with TB, particularly children with less severe disease at the primary healthcare level. Our CR readers had levels of expertise that are not generalizable to all clinicians across all clinical contexts. Further studies are needed to measure concordance between readers with varying levels of experience and expertise interpreting CRs taken in different settings and from diverse patient populations. As a closer proxy to CR interpretation in routine care settings, we used the CR data from single reads rather than a final consensus read. An additional consideration for this choice was that, although consensus-classified CRs have typically been standard in pediatric TB research, the process of reaching consensus is controversial and imperfect, and we are not aware of empirical evidence demonstrating that consensus read CRs have better accuracy than single-read CRs.

Although identifying CR features that are specific for pediatric TB is a major step forward, it would be important to evaluate these individual features in large prospective cohorts within the context of integrated diagnostic algorithms that combine clinical, radiological, and microbiological parameters. Our results have relevance for computer-aided detection (CAD) for TB on CR in children as the development of CAD algorithms will be reliant upon characterizing pediatric CRs in a systematic manner and establishing CR features that can distinguish TB from non-TB.

In conclusion, in the absence of a practical accurate diagnostic test for intrathoracic TB in children, a data-driven approach to CR classification is critical. Identifying the CR features that are specific for, and strongly associated with, TB can inform diagnosis and treatment decisions in routine care. We propose that using this more nuanced approach to CR interpretation in diagnostic algorithms, which consider the presence/absence of select CR features, will improve performance. The presence of specific CR features supports a diagnosis of intrathoracic TB, whereas their absence, without excluding the diagnosis, should

encourage clinicians to look for other supporting evidence of TB disease with consideration of an alternative diagnosis coupled with close clinical follow-up.

Supplementary Data

Supplementary materials are available at *Clinical Infectious Diseases* online. Consisting of data provided by the authors to benefit the reader, the posted materials are not copyedited and are the sole responsibility of the authors, so questions or comments should be addressed to the corresponding author.

Notes

Author contributions. M. P., J. A. S., and K. S. G. conceptualized this study. E. W. and A. C. H. conceptualized and designed the original diagnostic study. E. W., M. P., and M. M. v. d. Z. collected the data on the original diagnostic study. P. G., H. S. S., and J. M. interpreted the chest radiographs and provided input on the chest radiograph methodology. K. S. G., M. P., and J. A. S. analyzed and interpreted the data for this analysis. M. P. wrote this manuscript, and all authors reviewed it, provided input, and approved the final manuscript.

Acknowledgments. The authors acknowledge Professor Robert Gie for his role in this work—his direct contribution toward conceptualizing and supporting the original diagnostic cohort was significant but it is his compassionate mentorship of several of the authors that has ensured his work in the field of pediatric tuberculosis research maintains momentum.

Financial support. This work was supported by the Medical Research Council of South Africa, the Harry Crossley Foundation, the Faculty of Medicine and Health Science at Stellenbosch University, the South African National Research Foundation, the Foundation for Innovative New Diagnostics (to E. W.); the South African National Research Foundation's SARCHI Chair in Pediatric Tuberculosis (to E. W. and A. C. H.); the European and Developing Countries Clinical Trials Partnership supported by the European Union (TMA2019SFP-2836 TB lung-FACT2), the National Institute of Health Fogarty International Centre (K43TW011028) (to M. M. v. d. Z.); the UK Medical Research Council and the UK Department for International Development under the MRC/DFID Concordat agreement (MR/R007942/1) (to J. A. S.), the US National Institutes of Health through the Eunice Kennedy Shriver National Institute of Child Health and Human Development (F30HD105440), and through the Yale Medical Scientist Training Program (T32GM007205) (to K. S. G.). M. P., P. G., H. S. S., and J. M. have no relevant funding sources to declare.

Potential conflicts of interest. All authors: No reported conflicts of interest. All authors have submitted the ICMJE Form for Disclosure of Potential Conflicts of Interest. Conflicts that the editors consider relevant to the content of the manuscript have been disclosed.

References

1. WHO. Global tuberculosis report. World Health Oragnisation. **2021**. Available at: https://www.who.int/teams/global-tuberculosis-programme/data. Accessed 15 January 2022.
2. Muñoz-Sellart M, Yassin MA, Tumato M, Merid Y, Cuevas LE. Treatment outcome in children with tuberculosis in southern Ethiopia. Scand J Infect Dis **2009**; 41:450–5.
3. Cambanis A, Yassin MA, Ramsay A, Bertel Squire S, Arbide I, Cuevas LE. Rural poverty and delayed presentation to tuberculosis services in Ethiopia. Trop Med Int Health **2005**; 10:330–5.
4. Bonnet M, Nansumba M, Bastard M, et al. Outcome of children with presumptive tuberculosis in Mbarara, rural Uganda. Pediatr Infect Dis J **2018**; 37:147–52.
5. Beyers N, Gie RP, Schaaf HS, et al. Delay in the diagnosis, notification and initiation of treatment and compliance in children with tuberculosis. Tuber Lung Dis **1994**; 75:260–5.
6. Abubakar I, Laundy MT, French CE, Shingadia D. Epidemiology and treatment outcome of childhood tuberculosis in England and Wales: 1999–2006. Arch Dis Child **2008**; 93:1017–21.
7. Harausz EP, Garcia-Prats AJ, Law S, et al. Treatment and outcomes in children with multidrug-resistant tuberculosis: a systematic review and individual patient data meta-analysis. PLoS Med **2018**; 15:e1002591.
8. Dodd PJ, Yuen CM, Sismanidis C, Seddon JA, Jenkins HE. The global burden of tuberculosis mortality in children: a mathematical modelling study. Lancet Glob Health **2017**; 5:e898–906.
9. Graham SM, Ahmed T, Amanullah F, et al. Evaluation of tuberculosis diagnostics in children: 1. Proposed clinical case definitions for classification of intrathoracic tuberculosis disease. Consensus from an expert panel. J Infect Dis **2012**; 205:S199–208.
10. Newton SM, Brent AJ, Anderson S, Whittaker E, Kampmann B. Paediatric tuberculosis. Lancet Infect Dis **2008**; 8:498–510.
11. Graham SM, Cuevas LE, Jean-Philippe P, et al. Clinical case definitions for classification of intrathoracic tuberculosis in children: an update. Clin Infect Dis **2015**; 61:S179–87.
12. Gunasekera KS, Walters E, van der Zalm MM, et al. Development of a treatment-decision algorithm for human immunodeficiency virus-uninfected children evaluated for pulmonary tuberculosis. Clin Infect Dis **2021**; 73:e904–e12.
13. Marais BJ, Gie RP, Schaaf HS, et al. A proposed radiological classification of childhood intra-thoracic tuberculosis. Pediatr Radiol **2004**; 34:886–94.
14. Concepcion NDP, Laya BF, Andronikou S, et al. Standardized radiographic interpretation of thoracic tuberculosis in children. Pediatr Radiol **2017**; 47:1237–48.
15. Hesseling AC, Schaaf HS, Gie RP, Starke JR, Beyers N. A critical review of diagnostic approaches used in the diagnosis of childhood tuberculosis. Int J Tuberc Lung Dis **2002**; 6:1038–45.
16. Wiseman CA, Gie RP, Starke JR, et al. A proposed comprehensive classification of tuberculosis disease severity in children. Pediatr Infect Dis J **2012**; 31:347–52.
17. Jones C, Whittaker E, Bamford A, Kampmann B. Immunology and pathogenesis of childhood TB. Paediatr Respir Rev **2011**; 12:3–8.
18. Marais BJ, Gie RP, Schaaf HS, et al. The natural history of childhood intra-thoracic tuberculosis: a critical review of literature from the pre-chemotherapy era. Int J Tuberc Lung Dis **2004**; 8:392–402.
19. Marais BJ, Donald PR, Gie RP, Schaaf HS, Beyers N. Diversity of disease in childhood pulmonary tuberculosis. Ann Trop Paediatr **2005**; 25:79–86.
20. Schaaf HS, Marais BJ, Whitelaw A, et al. Culture-confirmed childhood tuberculosis in Cape Town, South Africa: a review of 596 cases. BMC Infect Dis **2007**; 7:140.
21. Frigati L, Maskew M, Workman L, et al. Clinical predictors of culture-confirmed pulmonary tuberculosis in children in a high tuberculosis and HIV prevalence area. Pediatr Infect Dis J **2015**; 34:e206–10.
22. Kaguthi G, Nduba V, Nyokabi J, Onchiri F, Gie R, Borgdorff M. Chest radiographs for pediatric TB diagnosis: interrater agreement and utility. Interdiscip Perspect Infect Dis **2014**; 2014:291841.
23. Berteloot L, Marcy O, Nguyen B, et al. Value of chest x-ray in TB diagnosis in HIV-infected children living in resource-limited countries: the ANRS 12229-PAANTHER 01 study. Int J Tuberc Lung Dis **2018**; 22:844–50.
24. Richter-Joubert L, Andronikou S, Workman L, Zar HJ. Assessment of airway compression on chest radiographs in children with pulmonary tuberculosis. Pediatr Radiol **2017**; 47:1283–91.
25. Massyn N, Peer N, English R, Padarath A, Barron P, Day C. District health barometer 2012/13. Durban, South Africa: Health Systems Trust, **2013**. Available at: https://www.hst.org.za/publications/District%20Health%20Barometers/DHB_2013_14_web.pdf. Accessed 27 January 2022.
26. Walters E, van der Zalm MM, Demers AM, et al. Specimen pooling as a diagnostic strategy for microbiologic confirmation in children with intrathoracic tuberculosis. Pediatr Infect Dis J **2019**; 38:e128–e31.
27. Gwet KL. Computing chance-corrected agreement coefficients (CAC). R package version 1.0. **2019**. Available at: https://cran.r-project.org/web/packages/irrCAC/vignettes/overview.html. Accessed 25 January 2022. .
28. Conway J. UpSetR: a more scalable alternative to venn and euler diagrams for visualizing intersecting sets. R package version 1.4.0. **2019**. Available at: https://rdrr.io/cran/UpSetR/. Accessed June 2021.
29. Swingler GH, du Toit G, Andronikou S, van der Merwe L, Zar HJ. Diagnostic accuracy of chest radiography in detecting mediastinal lymphadenopathy in suspected pulmonary tuberculosis. Arch Dis Child **2005**; 90:1153–6.